Common SNP in *pre-miR-146a* decreases mature miR expression and predisposes to papillary thyroid carcinoma

Krystian Jazdzewski*, Elizabeth L. Murray†, Kaarle Franssila‡, Barbara Jarzab§, Daniel R. Schoenberg†, and Albert de la Chapelle*¶

*Human Cancer Genetics Program, Comprehensive Cancer Center, Ohio State University, 850 Biomedical Research Tower, 460 West 12th Avenue, Columbus, OH 43210; †Department of Molecular and Cellular Biochemistry, Ohio State University, 366 Hamilton Hall, 1645 Neil Avenue, Columbus, OH 43210; ‡Department of Pathology, Helsinki University Central Hospital, FIN-00029, Helsinki, Finland; and §Department of Nuclear Medicine and Endocrine Oncology, Maria Sklodowska-Curie Memorial Cancer Center and Institute of Oncology, Wybrzeze Armii Krajowej 15, Gliwice 44-101, Poland

Contributed by Albert de la Chapelle, March 17, 2008 (sent for review February 12, 2008)

Although papillary thyroid carcinoma (PTC) displays strong heritability, no predisposing germ-line mutations have been found. We show that a common G/C polymorphism (rs2910164) within the pre-miR-146a sequence reduced the amount of pre- and mature miR-146a from the C allele 1.9- and 1.8-fold, respectively, compared with the G allele. This is matched by a similar decrease in the amount of each pre-miR generated from the corresponding pri-miR-146a in an *in vitro* processing reaction. The C allele also interfered with the binding of a nuclear factor to pre-miR-146a. The reduction in miR-146a led to less efficient inhibition of target genes involved in the Toll-like receptor and cytokine signaling pathway (TRAF6, IRAK1), and PTC1 (also known as CCDC6 or H4), a gene frequently rearranged with RET proto-oncogene in PTC. In an association study of 608 PTC patients and 901 controls, we found marked differences in genotype distribution of rs2910164 ($P = 0.000002$), the GC heterozygous state being associated with an increased risk of acquiring PTC (odds ratio = 1.62, $P = 0.000007$), and both homozygous states protective with odds ratio = 0.42 for the CC genotype ($P = 0.003$) and odds ratio = 0.69 for the GG genotype ($P = 0.0006$). Moreover, 4.7% of tumors had undergone somatic mutations of the SNP sequence. Thus, our data suggest that a common polymorphism in pre-miR-146a affects the miR expression, contributes to the genetic predisposition to PTC, and plays a role in the tumorigenesis through somatic mutation. Preliminary evidence suggests that these effects are mediated through target genes whose expression is affected by the SNP status.

genetic predisposition | microRNA processing | polymorphism | miR-146 | thyroid cancer

Papillary thyroid carcinoma (PTC) is the most common thyroid malignancy, accounting for ≈80% of all thyroid cancers. The incidence of PTC in the United States has increased in recent years and has reached ≈26,500 cases annually (1). The pathogenesis of PTC involves alterations in the RET/PTC-RAS-BRAF signaling pathway. Activating mutations in *BRAF* and *RET/PTC* gene rearrangements are frequent somatic changes in PTC tumors (2–6). A strong inherited genetic predisposition is suggested by case-control studies showing a 3- to 8-fold increase in risk in first-degree relatives, one of the highest risks of all cancers (7, 8). Despite unequivocal evidence of an inherited predisposition, large families displaying Mendelian inheritance of PTC are rare, and no predisposing genetic factors have been convincingly described, even though several putative loci have been identified by linkage analysis (9, 10).

MicroRNAs (miRs) are small noncoding RNA molecules that function as negative regulators of the expression of other genes; miRs inactivate specific mRNAs and interfere with the translation of target proteins (11). MicroRNAs are transcribed from endogenous DNA and form hairpin structures (called pre-microRNAs) that are processed to form mature microRNA duplexes that are ≈22 nucleotides long. A protein complex (called RNA-induced silencing complex; RISC) facilitates the coupling of one strand of the microRNA duplex with matching mRNA sequences in the 3′ untranslated regions of target genes; the other strand of the duplex is degraded. The binding of the microRNA to mRNA leads to inhibition of the translation of the latter, thus disrupting the expression of the protein. MicroRNAs regulate such major processes as development, apoptosis, cell proliferation, and hematopoiesis; they may act as tumor suppressor genes and oncomirs (12–14). The expression of miRNAs varies between cancer and normal cells and varies among different types of cancer (15, 16).

We reasoned that the previous failure to identify genes predisposing or contributing to PTC might be because these genes show low penetrance. The mechanisms may require the interaction of two or more genes; thus, regulatory, rather than protein-encoding, genes might be involved. MicroRNAs fulfill these criteria.

We and others have described several microRNAs showing transcriptional up-regulation in PTC tumors, the most striking being a 19-fold increase in the quantity of miR-146 (17, 18). Human *miR-146* occurs in two distinct forms: *miR-146a* encoded on chromosome 5q33 and *miR-146b* encoded on chromosome 10q24. Because the mature 22-mers differ by only 2 nt, many of the predicted target genes are common to both miRs, whereas, in addition, each is predicted to have specific targets unique to that miR. The two related *miR-146* are differentially regulated, with *miR-146a* (but not *miR-146b*) strongly induced by lipopolysaccharide. It is proposed that miR-146 has a role in Toll-like receptor and cytokine signaling and thus in the immune response, and there is evidence that *miR-146a* is regulated by NF-kappa B (19).

In an effort to elucidate the putative role of miR-146 in PTC we sequenced the *pri-miR-146a* and *pri-miR-146b* in the genomic DNA of those 15 patients whose samples had been analyzed for global miR expression (17). No previously undescribed sequence changes were detected. However, in the *pre-miR-146a* we noted a common G/C polymorphism designated rs2910164. It resides at position +60 relative to the first nucleotide of *pre-miR-146a*, placing it in the passenger strand (Fig. 1*A*). The rarer C allele causes mispairing within the hairpin and a lowering of the

Author contributions: K.J., D.R.S., and A.d.l.C. designed research; K.J. and E.L.M. performed research; K.J., K.F., and B.J. contributed new reagents/analytic tools; K.J., E.L.M., D.R.S., and A.d.l.C. analyzed data; and K.J., D.R.S., and A.d.l.C. wrote the paper.

The authors declare no conflict of interest.

¶To whom correspondence should be addressed. E-mail: albert.delachapelle@osumc.edu.

This article contains supporting information online at www.pnas.org/cgi/content/full/0802682105/DCSupplemental.

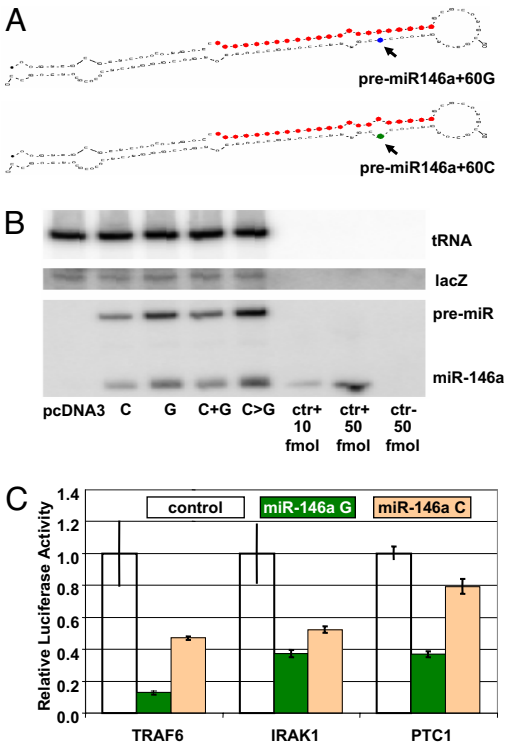

Fig. 1. Structure, expression, and inhibition of targets of miR-146a. (*A*) The predicted structure of pre-miR-146a. The location of the G/C SNP is shown by an arrow. The mature miR is shown by full red dots. (*B*) Northern blot. An oligo DNA complementary to mature miR-146a served as a probe. We loaded 20 μg of RNA from cells transfected with (*i*) empty vector, (*ii*) pcDNA3-miR-146a-C, (*iii*) pcDNA3-miR-146a-G, and (*iv*) 50% of each pcDNA3-miR-146a-G and pcDNA3-miR-146a-C (C+G). The lane labeled C>G describes an experiment where the expression of mature miR from the pcDNA3-miR-146a-C plasmid was reestablished by introducing the reverse mutation. The control lanes comprise 10 or 50 fmol of RNA oligo of the mature miR-146a (positive control for labeling by the Northern probe), and 50 fmol of RNA oligo complementary to the mature miR-146a (negative control). (*C*) Dual luciferase assay. The relative luciferase activity of reporter constructs with 3′ UTRs of TRAF6, IRAK1, and PTC1 containing legitimate (studied samples) or mutated (controls) target sites in the presence of miR-146a-C or miR-146a-G.

predicted ΔG from -43.1 kcal/mol to -40.3 kcal/mol (20). Sequence-mediated differences in processing have been reported for a viral miR (21) as well as for a human miR (22) and would have a quantitative impact on the total amount of miR-146a. The SNP might reduce the stability of the pri-miR, the efficiency of processing of pri-miR into pre-miR, or the efficiency of processing the pre-miR into the mature miR.

Results and Discussion

Expression of miR-146a in Transfected Cells. To investigate the functional impact of the SNP on the expression of miR-146a, we engineered an expression plasmid with 1,054 bp of pri-miR-146a with either G or C under the control of the CMV promoter. Plasmids were transfected (together with a plasmid expressing lacZ shRNA as a control of transfection efficiency) into a cell line (U2OS) that does not express the miR endogenously. Total RNA was extracted and assayed by Northern blot analysis with a probe for mature miR-146a (which is unaffected by the passenger strand polymorphism), for the LacZ shRNA, and for tRNA-Glu. The results were quantified by PhosphorImager analysis by using ImageQuant TL software (GE Healthcare), and normalized to both lacZ (transfection efficiency) and tRNA (loading amount). We noticed a relatively small variation in the transfection efficiency (coefficient of variation cv = 12.2%) and an even smaller variation of loading amount (cv = 6.8%). Pre-miR-146a and the mature miR were expressed from both alleles; however, the amount of each differed between the alleles. The expression of pre-miR-146a from the C allele was 1.9-fold lower than from the G allele, and the amount of mature miR-146a was 1.8-fold lower from the C allele compared to the G allele [Fig. 1*B* and supporting information (SI) Table S1]. Reduced expression of pre- and mature miR-146a was reversed by mutating the C back to G (Fig. 1*B*), thus indicating that this single nucleotide difference significantly alters the amount of miR-146a produced from the C allele. Importantly, the ratio of precursor-to-mature form was unchanged (2.2 and 2.1 for the G and C alleles, respectively), which makes it unlikely that this results from a block in Dicer processing. We conclude that the G>C substitution in pre-miR-146a results in reduced amounts of mature miR-146a.

Processing of pri-miR-146a. To determine whether the differences in Fig. 1 resulted from allele-specific differences in nuclear processing we examined the production of pre-miR-146a from the pri-miR in HeLa nuclear extract (23) (Fig. 2*A*). PhosphorImager analysis of products separated on a 12% denaturing polyacrylamide/urea gel showed that twice as much pre-miR-146a was generated from the G allele compared with the C allele, and a 1:1 mixture generated the anticipated mean of these two values. These results suggest that the 2-fold difference in miR-146a in Fig. 1 results from differences in nuclear processing. RNA electrophoretic mobility shift assay (EMSA) of nuclear protein binding to pre-miR-146a provided further evidence for differences between the two alleles (Fig. 2*B*). A retarded complex was formed when each of the pre-miRs was incubated on ice with HeLa nuclear extract (lanes 2 and 7); however, the complex assembled on pre-miR-146a-G was shifted further when an equal amount of the unlabeled pre-miR was added (compare lanes 3 and 8). This suggests that the amount of radiolabeled pre-miR-146a-G was below saturation, and increasing the amount of this RNA facilitated the formation of a specific complex. This binding was competed by a 5-fold excess of the homologous RNA, but not by a 5-fold excess of pre-miR-146a-C. These results indicate that the G/C polymorphism affects both the efficiency of pri-miR processing and protein binding to the pre-miR product of this reaction. The composition of the retarded complex was not examined further, but this may also affect the stability and/or efficiency of pre-miR-146a export to the cytoplasm.

Genetic Case-Control Association Study. To investigate whether the SNP in the pre-miR sequence was associated with the occurrence of PTC we studied genomic DNA from unselected, consecutive sporadic PTC patients (n = 608) and appropriate unaffected controls (n = 901). The samples emanated from Finland (206 cases, 274 controls), Poland (201 cases, 475 controls), and Ohio (201 cases, 152 controls); all participants were of Caucasian origin. We determined differences in distribution of genotypes between cancer patients and controls (combined $P = 0.000002$) with G/C heterozygosity being associated with an increased risk of acquiring PTC [odds ratio (OR) = 1.62, 95% C.I. 1.3–2.0, $P = 0.000007$; Table 1] in comparison with homozygosity. Both homozygous states were protective: OR = 0.42 for CC vs. GG+GC (95% CI 0.24–0.73, $P = 0.0027$), and OR = 0.69 for GG vs. CC+GC (95% CI 0.57–0.85, $P = 0.0006$), and OR = 0.5 for CC vs. GG (95% CI 0.28–0.89, $P = 0.024$). There was no difference in allelic frequency ($P = 0.15$). We also studied blood DNA from 191 patients with Graves' disease, a benign thyroid disorder, and found no association ($P = 0.22$), which suggests that the SNP is not unspecifically associated with any thyroid disease. We conclude that the germ-line genotype at the SNP affects the predisposition to PTC.

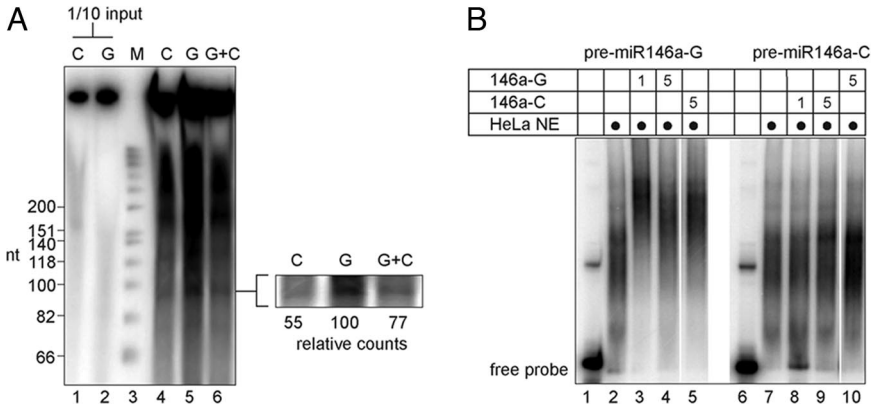

Fig. 2. Processing of pri-miR-146a. (*A*) *In vitro* processing assay. 1×10^5 dpm of gel-purified pri-miR-146a-C (lane 4) or G (lane 5) or a mixture of 0.5×10^5 cpm of each (lane 6) was incubated with HeLa nuclear extract for 90 min. After treating with proteinase K to digest nuclear proteins, radiolabeled RNAs were separated on a denaturing 12% polyacrylamide/urea gel and visualized by PhosphorImager. Lanes 1 and 2 contain 1×10^4 dpm of each input transcript and lane 3 contains a size ladder of radiolabeled HinfI cut ΦX174 DNA. The bands corresponding to pre-miR-146a are shown enlarged to the right of the autoradiogram, and the relative amount of radioactivity in each band normalized to the product of the G allele is shown beneath. (*B*) Electrophoretic mobility shift assay. Uniformly labeled transcripts of pre-miR-146a-G (lanes 1–5) or pre-miR-146a-C (lanes 6–10) were incubated for 30 min on ice without (lanes 1 and 6) or with 10 μg of HeLa nuclear extract (filled circles). The mixtures in lanes 3–5 and 8–10 were incubated for an additional 30 min with an equal amount or a 5-fold excess of each unlabeled pre-miR (indicated above the autoradiogram) before electrophoresis on a native 6% polyacrylamide gel. Retarded complexes were visualized by PhosphorImager analysis of the dried gel.

Somatic Mutations in PTC Tumors. We then determined the genotypes of PTC tumors. Tumor/normal tissue pairs were available from Finland ($n = 132$) and the United States ($n = 169$), but not from Poland. A most interesting observation was made in that the SNP underwent somatic mutations in tumor tissue. Of the 132 tumor/normal pairs from Finland, six cases had mutated from GG in the germ-line to GC in the tumor; two cases had mutated from CC to GC. In the U.S. series 5 GG genotypes had become GC and 1 CC had become GC (Fig. 3). Each tumor sample was cloned and individual PCR products genotyped. The frequency of clones exhibiting the mutation was 3–42% (Table S2). To exclude sample mismatching and confirm that both samples within a given tumor/normal pair derived from the same patient, we evaluated all discordant tumor/normal pairs with seven microsatellite markers similar to those used for identity testing by forensic laboratories (Table S3). To exclude mislabeling of tumor and normal samples within each pair, we checked tumor samples for the $BRAF^{V600E}$ mutation, which is a frequent somatic change in PTC tumors (5, 6). Ten of 14 tumor samples were positive and all normal samples were negative (Table S3). Thus, we found mutation from GG or CC in the germ-line toward GC heterozygosity in the tumor in 6.1% and 3.6% of tumor/normal tissue pairs from Finland and the United States, respectively. We conclude that the genotype at the SNP sustains somatic mutations in the tumors, a hallmark of cancer predisposition.

Expression of miR-146 in PTC Tumors. In our previous studies using a semiquantitative standard reverse transcription (RT)-PCR method we failed to show any expression of *miR-146a* in thyroid tumor samples (17). In this study, we repeated the evaluation of expression of both *miR-146a* and *miR-146b* by using the more sensitive Taqman "stem-loop" real-time RT-PCR in 9 PTC normal/tumor sample pairs, and found that both isoforms are expressed in normal thyroid and both are overexpressed in at least 7 of 9 PTC tumors. MiR-146a is 1.4- to 2.7-fold and miR-146b is 1.6- to 102-fold overexpressed in tumor samples compared with the unaffected part of the same gland (Table S4). In most cases of normal tissue, the expression of miR-146a is similar to or slightly higher than the expression of miR-146b; however, in six of nine tumor samples, the expression of miR-146a is at the level of 1–11% of the expression of miR-146b. Because of lack of DNA, we cannot correlate the expression of miR-146a and the SNP in the above nine samples. Instead, we evaluated the expression of mir-146a in a set of 33 lymphoblastoid cell lines derived from healthy individuals of known SNP status (Table S5). The mean expression of miR-146a in CC cases ($n = 3$) was 3.9-fold lower than the expression in 15 GG cases (Welch two-sample t test; $t = 3.1085$, df $= 14.88$, $P = 0.0073$), which confirmed the results of our transient transfection assay. Nevertheless, highly interestingly, the mean expression of miR-146a in GC ($n = 15$) cases was 1.4-fold higher than the expression in 15 GG cases. This result is not statistically significant ($t = -0.89$, df $= 22.26$, $P = 0.39$); however, it is similar to the results

Table 1. Genotype frequencies of *pre-miR-146a*+60G>C in three cohorts of PTC cases and controls

	Finland		Poland		USA		All	
	PTC $n = 206$	Controls $n = 274$	PTC $n = 201$	Controls $n = 475$	PTC $n = 201$	Controls $n = 152$	PTC $n = 608$	Controls $n = 901$
GG	99 (48.1%)	150 (55%)	115 (57.2%)	286 (60%)	91 (45.3%)	90 (59%)	305 (50.2%)	526 (58.4%)
GC	104 (50.5%)	105 (38%)	82 (40.8%)	163 (34%)	101 (50.2%)	52 (34%)	287 (47.2%)	320 (35.5%)
CC	3 (1.5%)	19 (7%)	4 (2%)	26 (5%)	9 (4.5%)	10 (7%)	16 (2.6%)	55 (6.1%)
		$P = 0.0017$		$P = 0.057$		$P = 0.01$		$P = 0.000002$

There was no difference in genotype frequencies between controls derived from Finland, Poland, and the United States ($P = 0.65$). Odds ratios were calculated for GC vs. GG + CC (OR = 1.62, 95% CI 1.3–2.0, $P = 0.000007$), CC vs. GG + GC (OR = 0.42, 95% CI 0.24–0.73, $P = 0.003$), GG vs. CC + GC (OR = 0.69, 95% CI 0.57–0.85, $P = 0.0006$), and CC vs. GG (OR = 0.5, 95% CI 0.28–0.89, $P = 0.024$). There was no difference in allelic distribution ($P = 0.15$).

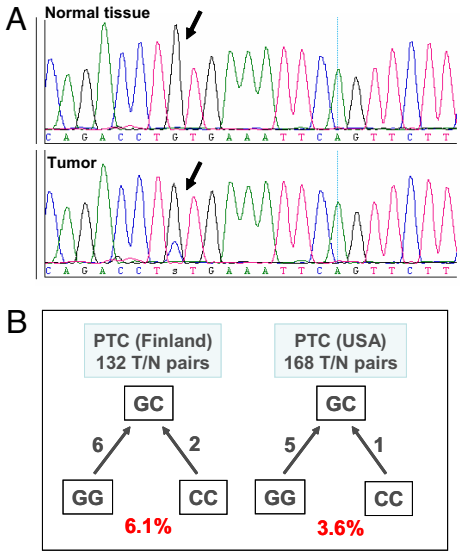

Fig. 3. Somatic mutations in tumor/normal tissue pairs. (*A*) An example of chromatographs showing a GG to GC mutation (arrow). (*B*) Summary of the numbers of cases showing different somatic mutations; arrows indicate direction from germ-line to tumor tissue.

in samples derived from the unaffected part of the thyroid from 11 additional PTC patients (CC is extremely rare among PTC patients and we had no such cases). In these 11 cases the mean expression of miR-146a in GC ($n = 6$) cases was 2.59-fold higher than the expression in 5 GG cases ($t = -1.03$, df $= 5.04$, $P = 0.35$; Table S6). Although the association data have high significance to show that GC heterozygosity predisposes to PTC, these experimental data will need further confirmation in larger series of cases and perhaps under varied conditions. Nevertheless, the results showing these subtle differences already lend support to the clinical association data. Thus, we are beginning to understand the unusual situation of an overdominant model in which heterozygosity constitutes the deleterious event rather than homozygosity for either allele.

Impact of SNP on miR-146a Target Genes. To initiate a study of the functional consequences of impaired processing of miR-146a on its target genes, we chose two proven target genes—IL-1 receptor-associated kinase 1 (*IRAK1*) and TNF receptor-associated factor 6 (*TRAF6*), key adapter molecules downstream of Toll-like and cytokine receptors—and one putative target gene—the papillary thyroid carcinoma 1 gene (*PTC1* also known as *CCDC6* or *H4*) that is frequently rearranged by translocation with the *RET* proto-oncogene in PTC (Fig. S1). We generated reporter constructs that contained the firefly luciferase gene fused to ≈150 bp of the 3′ UTRs from IRAK1, TRAF6, and PTC1 mRNAs containing miR-146a putative target sites (IRAK1-luc, TRAF6-luc, and PTC1-luc, respectively). Plasmids with inserts carrying mutations of 4 nt in the miR-146a target sequences served as controls (Fig. S2). These reporter constructs were transiently transfected into U2OS cells together with an expression plasmid for either miR-146a-G or miR-146a-C under the control of the CMV promoter. We ran all samples in triplicate and replicated the experiment twice. We observed a marked reduction in luciferase levels in cells coexpressing miR-146a together with IRAK1-luc, TRAF6-luc, and PTC1-luc; moreover, the reduction was much stronger in the presence of miR-146a-G than miR-146a-C (Fig. 1*D*). This suggests a direct functional effect of the SNP.

Conclusions. Our data show that a common polymorphism in *pre-miR-146a* affects the amount of mature miR, contributes to the genetic predisposition to PTC, and plays a role in the tumorigenesis through somatic mutation. Preliminary evidence suggests that these effects are mediated through target genes whose expression is affected by the SNP status. Because miR-146a is known to be a NF-kappa B-dependent gene (24, 25) and does inhibit *TRAF6* and *IRAK1*, key adapter molecules downstream of the Toll-like and cytokine receptors, we hypothesize a role for the SNP in affecting the negative feedback regulation loop in the Toll-like receptor and cytokine signaling pathway. The NF-kappa B pathway is critical for tumor formation because it promotes not only cell survival by the expression of antiapoptotic proteins, but also the transcription of many immune-related genes and proinflammatory cytokines that can influence tumor progression through the mobilization of host cells (26). The role of Toll-like receptors and NF-kappa B in thyroid tumorigenesis is well established (27–29) and it was recently reported that $BRAF^{V600E}$, the common somatic mutation in PTC tumors, promotes invasiveness of thyroid cancer cells through NF-kappa B (30). We believe that our findings create an opportunity to approach the diagnosis and treatment of PTC.

Materials and Methods

Patient and Control Samples. After approval of the Institutional Review Board and patient consent, fresh samples from PTC tumor tissue and normal thyroid tissue adjacent to PTC tumors were obtained from patients with sporadic PTC undergoing surgical resection; the samples were snap-frozen in liquid nitrogen and stored at −80°C (Finland and United States). Alternatively, formalin-fixed, paraffin-embedded material was used. Other samples included blood DNA samples of Polish PTC patients; blood DNA samples of random Finnish, Polish, and American control individuals; and blood DNA samples of Polish Graves disease patients.

Nucleic Acid Extraction. DNA was extracted by standard methods. Total RNA was extracted from cell lines with TRIzol solution (Invitrogen), and the integrity of RNA was assessed by using an Agilent BioAnalyzer 2100 (Agilent).

Sequencing. DNA specimens were amplified by using standard PCR protocols. The PCR products were purified with ExoSAP-IT purification kit (USB Corp.) and sequenced in both directions with the ABI sequencing system (PerkinElmer Applied Biosystems). The sequencing results were analyzed by using DNAStar SEQMAN software. The PCR primers used for *miR-146a* sequencing were: 5′-ATT TTA CAG GGC TGG GAC AG-3′ and 5′-TCT TCC AAG CTC TTC AGC AG-3′. In addition to sequencing, the SNP was genotyped by using the Single Nucleotide Primer Extension Assay (ABI PRISM SNaPshot Multiplex Kit, Applied Biosystems) in about half of the samples. All results were concordant. The PCR primers used for the $BRAF^{V600E}$ sequencing were: 5′-TGC TTG CTC TGA TAG GAA AAT G-3′ and 5′-CCA CAA AAT GGA TCC AGA CA-3′.

Statistical Analysis. Statistical analysis was conducted by using R software (http://cran.r-project.org) with additional packages ''survival'' and ''genetics.'' The χ^2 test was applied to check the homogeneity in genotype frequency distributions between the patient group and controls. If any of the expected counts was <5, the Fisher's exact test was applied. A P value of <0.05 was considered statistically significant. Genotype frequencies in all groups were checked for the Hardy–Weinberg equilibrium by using the χ^2 test. Odds ratios were calculated by Woolf's method. A t test was used to compare differences in mean expression levels between groups of samples in real-time RT-PCR experiment.

MiR-146a Expression Vectors and U2OS Cell Transfection. To create pre-miR-146a+60G and pre-miR-146a+60C expression vectors genomic fragments (1,054 bp) corresponding to pre-miR and its flanking regions were amplified from human genomic DNA (previously determined to have the GG or CC genotype) and cloned into the vector pcDNA3 (Invitrogen). The sequences of both vectors were confirmed by direct sequencing; the only difference was in the SNP. U2OS cells were plated at 2.2×10^6 cells per 100-mm dish and transfected 24 h later by using FuGENE6 reagent (Roche). Each transfection reaction contained 500 ng of pcDNA3-146a-G or 500 ng of pcDNA3-146a-C or 250 ng of both plus 500 ng of pENTR/H1/TO expressing lacZ shRNA (Invitrogen). The sequence of the lacZ shRNA transcript was as follows: 5′-

AAATCGCTGATTTGTGTAGTCGGAGACGACTACACAAATCAGCGAUUU-3′. As controls we performed mock transfection (no plasmids), transfection with empty plasmid (pcDNA only), and used untransfected cells. Total RNA was extracted 24 h after transfection and used for Northern blot analysis and real-time RT-PCR.

Northern Blot Analysis of miR-146a. Twenty micrograms of total RNA was loaded onto a precast 15% denaturing TBE-urea polyacrylamide gel (Bio-Rad). The RNA was then electrophoretically transferred to Bright-Star blotting membranes (Ambion). The oligonucleotides used as probes were the complementary sequence of the mature miR-146a (5′-AAC CCA TGG AAT TCA GTT CTC A-3′), miR-146b (5′-AGC CTA TGG AAT TCA GTT CTC A-3′), and tRNA (5′-GCG GCG GTG AGA GCG CCG AAT C-3′) with Starfire modification (Integrated DNA Technologies). Probes were end-labeled with [α-^{32}P]dATP by using the StarFire Oligonucleotide Labeling System (Integrated DNA Technologies). Prehybridization and hybridization were carried out in Ultrahyb Oligo solution (Ambion) containing at least 10^6 cpm/ml of probe overnight at 37°C. After washing (three times for $\times$ 5 min with 2$\times$ SSC/0.1% SDS at 42°C) the membrane was exposed to phosphor screen and an image was produced by using STORM-SCANNER and ImageQuant TL software (GE Healthcare). For a loading control, the blots were stripped by boiling and reprobed by using the 22-nt sequence complementary to tRNA-Glu (5′-GCG GCG GTG AGA GCG CCG AAT C-3′). For a transfection control, the blots were reprobed by using the 19-nt sequence complementary to lacZ shRNA (5′-TCG CTG ATT TGT GTA GTC G-3′).

Real-Time RT-PCR Detection of miR-146a. To evaluate the *miR-146a* and *mir-146b* expression levels, ''stem-loop'' real-time RT-PCR was used. RNA (100 ng) was used for RT reactions that were performed by using High Capacity cDNA Reverse Trancription Kit (Applied Biosystems) according to the manufacturer's protocol. Real-time PCR was performed on the ABI Prism 7900HT Sequence Detection System. U6 RNA was used as an endogenous control. All primers were part of Taqman MicroRNA Assays for *miR-146a*, *miR-146b*, or RNU6B (Applied Biosystems). The cycle number at which the product level exceeded an arbitrarily chosen threshold (C_T) was determined for each target sequence, and the amount of each miR relative to U6 RNA was described by using the formula $2^{-\Delta C_T}$, where $\Delta C_T = C_{T(\text{miR})} - C_{T(\text{U6 RNA})}$.

Hybridization Prediction. The minimum free-energy hybridization of miRNAs and target mRNA were predicted by RNAHYBRID software freely available at http://bibiserv.techfak.uni-bielefeld.de/rnahybrid.

3′ UTR Luciferase Reporter Assays. To generate 3′ UTR luciferase reporter constructs ≈150 bp of the 3′ UTRs from IRAK1, TRAF6, and PTC1 mRNAs were cloned downstream of the firefly luciferase gene in pGL3-Control Vector (Promega). Mutated control vectors carrying 4-bp substitutions in the miR-146 target sites were obtained by PCR and degenerated primers. For luciferase reporter assays, U2OS cells were plated at 0.2×10^6 cells per well in 12-well dishes and 24 h later cotransfected with FuGENE6 reagent (Roche). Each cotransfection reaction contained 200 ng of pcDNA3-146a-G or 200 ng of pcDNA3-146a-C plus 200 ng of pGL3-3′UTR construct plus 20 ng of pRL-TK plasmid that served as transfection control. After 24 h, cells were washed and lysed with Passive Lysis Buffer (Promega), and their firefly luciferase activity was measured by using the Veritas Microplate Luminometer (Turner Biosystems) and normalized to renilla luciferase activity. We ran all samples in triplicate and replicated the experiment twice.

Cloning of Reverse Mutation in pre-miR-146a-C. HPLC-purified and 5′-phosphorylated primers 5′P-ACA ACC CAT GGA ATT CAG TTC TCA AAG C-3′ and 5′P-GTC AGT GTC AGA CCT GTG AAA TTC AGT TC-3′ were used to introduce a C-to-G mutation in pri-miR-146a-C by PCR. PCR products were ligated and cloned by using the Phusion site-directed mutagenesis kit (Finnzymes). Constructs were verified by sequencing.

Cloning of Plasmids for *in Vitro* Transcription Templates. Primers 5′-GCC GAT GTG TTA TCC TCA GCT TTG-3′ and 5′-ACG ATG ACA GAG ATA TCC CAG-3′ were used to amplify pre-miR-146a-C or pre-miR-146a-G from plasmids pcDNA3-miR-146a-C or pcDNA3-miR-146a-G, respectively, by PCR. PCR products were ligated into pCRII-TOPO to create plasmids pCRII-pre-miR-146a-C and pCRII-pre-miR-146a-G and constructs were confirmed by DNA sequencing.

***In Vitro* Transcription.** Internally labeled *in vitro* transcripts were produced by using the MAXIscript *in vitro* transcription kit (Ambion) and [α-^{32}P]dATP. For the UV cross-linking experiment in Fig. 2*A*, plasmids pCRII-pre-miR-146a-C and pCRII-pre-miR-146a-G were linearized by BamHI digestion, and *in vitro* transcripts were generated with T7 RNA polymerase. For the *in vitro* processing experiment in Fig. 2*B* the ApaI-linearized pri-miR expression plasmids pcDNA3-146a-GΔPL or pcDNA3-146a-CΔPL were transcribed by using T7 RNA polymerase. *In vitro* transcripts were purified by electrophoresis on a denaturing 6% or 4% polyacrylamide/urea gels, respectively, and bands visualized by autoradiography were cut out and eluted from the gels. The eluted RNA was extracted with phenol/chloroform/isoamyl alcohol and recovered by ethanol precipitation. The quality and specific activity of each transcript was then determined.

Electrophoretic Mobility Shift Assay. One hundred femtomoles of uniformly labeled *in vitro* transcripts of pre-miR-146a-C or pre-miR-146a-G was mixed with 10 μg of HeLa nuclear extract in buffer containing 2 mM Tris·HCl, pH 7.6, 0.2 mM $Mg(OAc)_2$, 0.2 mM DTT, 14 mM KCl, 2% glycerol, 0.2 mM EDTA, 3 μM EGTA, and 550 ng/μl heparin. The reaction mixtures were incubated on ice for 30 min, followed by addition of the indicated fold excess of unlabeled pre-miR146a-C/G *in vitro* transcript and further incubation on ice for 30 min. Samples were electrophoresed at 200 V and 4°C for 3.5 h on a 6% native polyacrylamide gel (acrylamide/bisacrylamide 40:1) in 1$\times$ Tris-acetate-EDTA (TAE). The gel was dried to Whatman paper and visualized by phosphorimager.

***In Vitro* Processing of pri-miR-146a.** *In vitro* processing reactions were performed as described in ref. 23. Each reaction contained 5 μl of HeLa nuclear extract, 1 μl of RNA (1×10^5 dpm), 1 μl of buffer A (32 mM $MgCl_2$, 5 mM ATP, 200 mM creatine phosphate), and water to 10 μl. These mixtures were incubated for 90 min at 37°C; the reaction was terminated by placing the tubes on ice and adding 2 μl of 20 mg/ml proteinase K. This mixture was incubated for 20 min at 63°C followed by addition of an equal volume of formamide dye loading buffer. The mixture was heated for 5 min at 100°C, separated on a denaturing 15% polyacrylamide/urea gel and visualized by phosphorimager.

ACKNOWLEDGMENTS. We thank Huiling He and George A. Calin for valuable advice. This work was supported by National Cancer Institute Grant P30 CA16058 (to the Ohio State University Comprehensive Cancer Center), a Thy-Ca Research Grant from the American Thyroid Association (to K.J.), and Public Health Service National Institute of General Medical Science Grant GM38277 (to D.R.S.), and MNil Grant 2P05A02230 (to B.J). K.J. received the Abbott Thyroid Research Clinical Fellowship Award presented by the Endocrine Society.

1. Jemal A, *et al.* (2007) Cancer statistics 2007. *CA Cancer J Clin* 57:43–66.
2. Grieco M, *et al.* (1990) PTC is a novel rearranged form of the ret proto-oncogene and is frequently detected in vivo in human thyroid papillary carcinomas. *Cell* 60:557–563.
3. Bongarzone I, *et al.* (1994) Frequent activation of ret protooncogene by fusion with a new activating gene in papillary thyroid carcinomas. *Cancer Res* 54:2979–2985.
4. Cohen Y, *et al.* (2003) BRAF mutation in papillary thyroid carcinoma. *J Natl Cancer Inst* 95:625–627.
5. Fukushima T, *et al.* (2003) BRAF mutations in papillary carcinomas of the thyroid. *Oncogene* 22:6455–6457.
6. Kimura ET, *et al.* (2003) High prevalence of BRAF mutations in thyroid cancer: Genetic evidence for constitutive activation of the RET/PTC-RAS-BRAF signaling pathway in papillary thyroid carcinoma. *Cancer Res* 63:1454–1457.
7. Goldgar DE, Easton DF, Cannon-Albright LA, Skolnick MH (1994) Systematic population-based assessment of cancer risk in first-degree relatives of cancer probands. *J Natl Cancer Inst* 86:1600–1608.
8. Czene K, Lichtenstein P, Hemminki K (2002) Environmental and heritable causes of cancer among 9.6 million individuals in the Swedish Family-Cancer Database. *Int J Cancer* 99:260–266.
9. Canzian F, *et al.* (1998) A gene predisposing to familial thyroid tumors with cell oxyphilia maps to chromosome 19p13.2. *Am J Hum Genet* 63:1743–1748.
10. McKay JD, *et al.* (2001) Localization of a susceptibility gene for familial non-medullary thyroid carcinoma to chromosome 2q21. *Am J Hum Genet* 69: 440–446.
11. Bartel DP (2004) MicroRNAs: Genomics, biogenesis, mechanism, and function. *Cell* 116:281–297.
12. Croce CM, Calin GA (2005) miRNAs, cancer, and stem cell division. *Cell* 122:6–7.
13. Esquela-Kerscher A, Slack FJ (2006) Oncomirs—microRNAs with a role in cancer. *Nat Rev Cancer* 6:259–269.
14. Zhang B, *et al.* (2007) microRNAs as oncogenes and tumor suppressors. *Dev Biol* 302:1–12.
15. Lu J, *et al.* (2005) MicroRNA expression profiles classify human cancers. *Nature* 435:834–838.
16. Calin GA, Croce CM (2006) MicroRNA signatures in human cancers. *Nat Rev Cancer* 6:857–866.
17. He H, *et al.* (2005) The role of microRNA genes in papillary thyroid carcinoma. *Proc Natl Acad Sci USA* 102:19075–19080.

18. Pallante P, *et al.* (2006) MicroRNA deregulation in human thyroid papillary carcinomas. *Endocr Relat Cancer* 13:497–508.
19. Taganov KD, Boldin MP, Chang K-J, Baltimore D (2006) NF-kB-dependent induction of microRNA miR-146, an inhibitor targeted to signaling proteins of innate immune responses. *Proc Natl Acad Sci USA* 103:12481–12486.
20. Rehmsmeier M, Steffen P, Hochsmann M, Giegerich R (2004) Fast and effective prediction of microRNA/target duplexes. *RNA* 10:1507–1517.
21. Gottwein E, Cai X, Cullen BR (2006) A novel assay for viral microRNA function identifies a single nucleotide polymorphism that affects Drosha processing. *J Virol* 80:5321–5326.
22. Duan R, Pak C, Jin P (2007) Single nucleotide polymorphism associated with mature miR-125a alters the processing of pri-miRNA. *Hum Mol Genet* 6:1124–1131.
23. Lee Y, Jeon K, Lee J-T, Kim S, Kim VN (2002) MicroRNA maturation: Stepwise processing and subcellular localization. *EMBO J* 21:4663–4670.
24. Taganov KD, Boldin MP, Baltimore D (2007) MicroRNAs and immunity: Tiny players in a big field. *Immunity* 26:133–137.
25. Cameron JE, *et al.* (2008) Epstein-Barr virus latent membrane protein 1 induces cellular microRNA miR-146a, a modulator of lymphocyte signaling pathways. *J Virol* 82:1946–1958.
26. Karin M, Lin A (2002) NF-kappaB at the crossroads of life and death. *Nat Immunol* 3:221–227.
27. Visconti R, *et al.* (1997) Expression of the neoplastic phenotype by human thyroid carcinoma cell lines requires NFkappaB p65 protein expression. *Oncogene* 15:1987–1994.
28. Pacifico F, *et al.* (2004) Oncogenic and anti-apoptotic activity of NF-kappa B in human thyroid carcinomas. *J Biol Chem* 279:54610–54619.
29. McCall KD, *et al.* (2007) High basal levels of functional toll-like receptor 3 (TLR3) and noncanonical Wnt5a are expressed in papillary thyroid cancer and are coordinately decreased by phenylmethimazole together with cell proliferation and migration. *Endocrinology* 148:4226–4237.
30. Palona I, *et al.* (2006) BRAFV600E promotes invasiveness of thyroid cancer cells through nuclear factor kappaB activation. *Endocrinology* 147:5699–5707.